microorganisms

MDPI

Article

Transplantation-Driven Microbial Shifts and Keystone Taxa Enhance Medicinal Ingredients in *Astragalus mongholicus*

Yanmei Li [1,2], Jiangying Huang [1], Xinrui Wang [1], Chenyuan Wang [1], Gehong Wei [1] and Zhefei Li [1,*]

[1] State Key Laboratory for Crop Stress Resistance and High-Efficiency Production, College of Life Science, Northwest A&F University, Xianyang 712100, China
[2] College of Veterinary Medicine, Southwest University, Beibei District, Chongqing 400715, China
* Correspondence: lizhefei@nwafu.edu.cn; Tel.: +86-29-87081416; Fax: +86-29-87092262

Abstract

Root-associated microbes play a crucial role in plant growth, stress resistance and the accumulation of secondary metabolites. In this study, LC-MS analysis revealed that soil provenance exerts a decisive influence on the content of flavonoids and astragalosides in *Astragalus membranaceus*. Transplant assays revealed that each soil type acted as a selective filter, assembling distinct microbial communities in both the rhizosphere and root of *Astragalus membranaceus*. The rhizosphere taxa selected from Yangling soil specifically enhanced flavonoid levels, whereas the root taxa selected from TanChang soil drove higher astragaloside accumulation. SourceTracker revealed that seedling root-endosphere ASVs served as the primary inoculum for later communities, confirming strong priority effects among early colonizers. Keystones tightly linked to both metabolite contents and biomass belonging to *Caulobacteraceae*, *Acidimicrobiia*, *Sutterellaceae*, *Bradyrhizobium*, *Sphingomonas* and *Mesorhizobium* were isolated, and the SynComs were constructed. In Tanchang soil, SynComs inoculation raised Astragaloside IV (AST IV) and Calycosin-7-glucoside (CAG) contents by 52.30% and 55.73%, respectively; in Yangling soil, the same consortium increased Astragaloside I (AST I), Astragaloside II (AST II), AST IV and CAG by 29.38%, 39.04%, 54.97% and 58.98% compared to the uninoculated controls. Collectively, our work charts the transplantation-driven dynamics of root-associated bacterial communities and medicinal metabolites, pinpoints keystones that govern ingredient accumulation and delivers validated microbial strains for enhancing the quality and pharmaceutical value of *Astragalus mongholicus*.

Keywords: root-associated microbes; medicinal ingredients; synthetic bacteria community; keystone taxa; priority effects

Check for updates

Academic Editor: Mohamed Hijri

Received: 10 December 2025
Revised: 30 January 2026
Accepted: 5 February 2026
Published: 12 February 2026

Copyright: © 2026 by the authors. Licensee MDPI, Basel, Switzerland. This article is an open access article distributed under the terms and conditions of the Creative Commons Attribution (CC BY) license.

1. Introduction

The root-associated compartments, primarily the rhizosphere and endosphere, are distinctive micro-habitats that differ markedly from bulk soil and serve as a major reservoir of plant-associated microorganisms [1]. These microorganisms underpin growth, fitness and productivity by shielding plants from biotic [2–5] and abiotic stresses [6–8]. As the composition, diversity and ecological functions of these microbial communities become clearer, harnessing the crop microbiota is becoming an important strategy for sustainable agriculture [9].

Although root-associated microbiota do not all perform identical roles in plant–microbe interactions, specific beneficial taxa have been shown to suppress pathogens [10],

accelerate nutrient cycling [7] and stimulate secondary metabolite accumulation [11]. However, these benefits are often undermined by low colonization rates and fierce competition with indigenous microbes [12]. Fecal microbiota transplantation, now adapted to plants, offers a fresh, disease-modifying toolkit to overcome these hurdles [13], yet owing to logistical bottlenecks in donor selection, microbe preservation and field delivery, this strategy remains largely untapped in crop systems. Transplanting whole, functional rhizosphere consortia from stress-resistant donors to susceptible receivers is now emerging as a practical route to re-assemble protective microbiomes and durably enhance plant health [14]. Overall, transplanting root-associated microbiota offers fresh insight into how root microbial communities arise and assemble.

Soil is widely regarded as a "microbial seed bank" that supplies plants with a vast pool of candidate symbionts [15]; not surprisingly, roots selectively recruit distinct taxa from contrasting edaphic backgrounds to meet their metabolic and defensive demands [16,17]. Microbial colonization of plants is governed by "priority effects": early arrivals alter the niche in ways that either facilitate or impede later immigrants [18]. This principle has been documented across plant tissues [19,20] and soils [21]. Early arrivals sequester, limiting carbon and occupying prime niches, erecting a barrier that later immigrants must overcome. In a landmark experiment, Carlstrom et al. [19] demonstrated that merely shuffling the inoculation order of 62 native bacterial strains produced historically contingent communities whose composition diverged sharply from random expectations. When these priority-shaped consortia are transplanted into new environments or exposed to sudden stress, the founding taxa re-assemble into configurations that either buffer the shock [22] or endow the community with novel metabolic capabilities [23]. Strains that repeatedly persist through environmental shifts thanks to priority-established dominance are therefore emerging as prime genetic resources for targeted microbiome engineering.

Synthetic communities (SynComs) have moved plant microbiome engineering beyond the "one-strain-at-a-time" era and now provide a powerful platform for improving plant performance [9,24]. These mini-ecosystems are designed around empirically detected microbial interactions [25]: they typically combine (i) high-abundance core taxa shared across samples, (ii) keystone species identified by co-occurrence network analyses and (iii) taxa whose abundance significantly differs between treatments [26]. SynComs are now routinely deployed to suppress disease [9,10], raise crop yields [27] and dissect the ecological rules shaping microbiomes [26,28]. In medicinal plants, tailored consortia have been shown to boost both the biomass and bioactive metabolite content of *Salvia miltiorrhiza* by reprogramming the host's secondary metabolism pathways [29].

Astragalus membranaceus (Fisch.) Bunge var. *mongholicus* (hereafter *Astragalus*) is a leguminous medicinal herb and high-value cash crop native to arid and semi-arid regions of China [30]. The chemical profile of *A. mongholicus* is dominated by two major classes of bioactive compounds, astragalosides and flavonoids, which have been widely used to enhance immunity, regulate metabolism and treat cardiovascular and respiratory disorders [31]. In this study, six compounds (AST I, II, III, IV, calycosin (CA) and formononetin (FO)) were chosen for quantification due to three key reasons. First, these compounds are officially listed in the Chinese Pharmacopoeia as quality control markers for *A. mongholicus*, with minimum content requirements for medicinal use. Second, previous studies have shown that their accumulation is closely associated with environmental factors (e.g., soil nutrients and climate) and microbial communities [11,32]. Third, they represent distinct biosynthetic pathways (mevalonate pathway for astragalosides and phenylpropanoid pathway for flavonoids), allowing us to evaluate the broader impact of microbial communities on plant secondary metabolism. By focusing on these core medicinal ingredients, this study provides direct insights into how transplantation-induced microbial shifts affect the

pharmaceutical value of *A. mongholicus*, which is critical for guiding sustainable cultivation practices and improving product quality.

In agricultural practice, *Astragalus* is routinely produced by transplantation, a method that shortens the growth cycle, increases survival and markedly boosts root yield. However, the impact of transplantation on the composition and function of preferential microbial colonizers, and the subsequent effects on medicinal ingredient accumulation, remains poorly understood. To address this gap, an indoor pot experiment mimicking field transplantation of *Astragalus* was conducted to (i) evaluate how transplantation reshapes root-associated microbial communities and affects the content of flavonoids and astragalosides; (ii) determine whether microbes that establish through priority effects can continue to colonize the rhizosphere when confronted with a new resident microbial community after transplantation; and (iii) reconstruct a synthetic community from identified keystone strains and verify its ability to boost the accumulation of medicinal ingredients in *Astragalus*.

2. Materials and Methods

2.1. Sampling Sites and Soil Collection

The topsoil (0–20 cm) used in this experiment was collected from Hunyuan County, Shanxi Province (39°32′ N, 113°35′ E), and Tanchang County, Gansu Province (34°17′ N, 104°10′ E), both with a long history of *Astragalus* cultivation. Yangling District, Shaanxi Province (34°16′ N, 108°46′ E), where the *Astragalus* has never been planted, served as the non-cultivation control. At each site, surface debris was removed before sampling; soils were immediately sieved (2 mm) to eliminate stones and root fragments, transported on ice and stored at 4 °C until use.

2.2. Pot Experiment Design

Vermiculite was thoroughly mixed with soil at a 1:3 ratio, and 1.8 kg of the resulting mixture was placed into each pot (18 cm diameter × 20 cm height) for subsequent experiments (experimental layout shown in Figure 1). The detailed potting design and sampling details can be found in the Supplementary Materials. Briefly, *Astragalus* seeds were surface-sterilized according to Li et al. [10], germinated on sterile Petri dishes and incubated until radicles emerged. Three-day-old seedlings of uniform size were transferred to pots containing soil collected from Tanchang County, adjusted to 30% of maximum field water capacity. Pots were kept in a greenhouse under a 16/8 h photoperiod (day/night temperature 20–25 °C) for 30 days. After this pre-culture period, seedlings were carefully uprooted with roots kept intact and transplanted into pots containing either Hunyuan soil (SHY) or Yangling soil (SYL). Those transplanted into Tanchang soil (STC) were used as the control. Rhizosphere and root samples were harvested 30 (T1), 60 (T2) and 90 (T3) days post-transplant following the method of Edwards et al. [33]. Concurrently, plant growth parameters (root and shoot length, and fresh and dry weights) were recorded at each sampling time point. A total of 120 samples were collected, and the sampling design is detailed in Table S1, including 60 rhizosphere samples and 60 root samples.

2.3. DNA Extraction and Sequencing

Soil DNA from a 0.5 g portion of rhizosphere soil was extracted with the Fast DNA Spin Kit for Soil (MP Biomedicals, Solon, CA, USA) according to the manufacturer's instructions. The root samples were freeze-dried for 48 h and homogenized in liquid nitrogen. DNA was then extracted from 50 mg portions of the root samples using the Power Plant DNA Isolation kit (MoBIo, Carlsbad, CA, USA) according to the manufacturer's protocol. DNA concentration and purity were quantified using a NanoDrop 2000 spectrophotometer (Thermo Scientific, Waltham, MA, USA) and agarose gel electrophoresis (1% agarose).

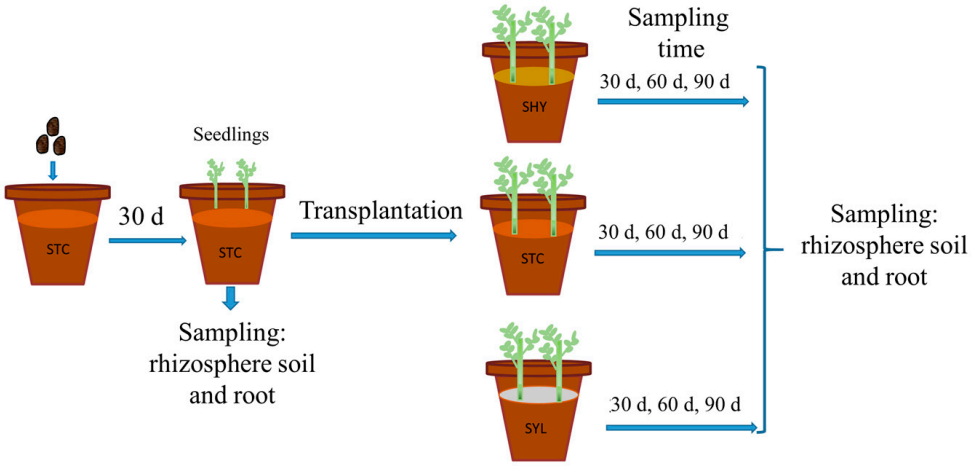


Figure 1. A schematic of the experimental design. Seeds were sown in soil from Tanchang County (STC); after 30 d, the seedlings and their adhering rhizosphere soil were transplanted into the soil from Hunyuan County (SHY), Yangling District (SYL) and Tanchang County (STC). Rhizosphere and root samples were collected at 30, 60 and 90 days after transplantation.

The bacterial V5–V7 region of the 16S rRNA gene was amplified using the primer pair 799F (5′-AACMGGATTAGATACCCKG-3′) and 1193R (5′-ACGTCATCCCCACCTTCC-3′) [34]. PCR was performed in a 50 µL reaction mixture comprising 0.5 µL of each primer (50 pmol), 25 µL of 2.5X Hot Master Mix (5-primer), 2 µL of DNA template and 22 µL of sterile water. The PCR conditions were as follows: 94 °C for 2.5 min (initial denaturation), followed by 30 cycles of 94 °C for 30 s (denaturation), 55 °C for 40 s (annealing) and 68 °C for 40 s (extension), and a final extension step of 68 °C for 7 min. The PCR products obtained in triplicate for each sample were pooled and purified using the Qiagen Gel Extraction Kit (Qiagen, Hilden, Germany). Sequencing libraries were generated using the Ion plus Fragment Library Kit 48 reactions (Thermo Scientific, Waltham, MA, USA) according to the manufacturer's recommendations. The library quality was assessed using a Qubit 2.0 Fluorometer (Thermo Scientific, Waltham, MA, USA). Finally, the library was sequenced on the PE250 IIumina NovaSeq platform, and 250 bp double-end reads were generated at the Novogene Bioinformatics Technology Co., Ltd. (Beijing, China).

Raw Illumina reads were processed with the DADA2 pipeline in R [35]. The following parameters were used: forward reads were truncated at 240 bp and reverse reads at 160 bp; maximum expected errors were set to 2 for forward reads and 2 for reverse reads; and paired reads were merged with a minimum overlap of 10 bp; chimeras were removed using the "consensus" method. ASVs were obtained, and representative sequences were classified against the SILVA 138 database [36] using the RDP classifier with a confidence threshold of 0.8. Sequences annotated as chloroplast, mitochondrial or non-bacterial were discarded [37]. The ASV abundance in all the samples was normalized using at least one sequence in two samples [38], and all downstream analyses were performed on this normalized data set.

2.4. Tracking the Origin of Post-Transplant Microbiota

To identify which bacterial lineages introduced at the seedling stage still drive community composition and metabolite quality after transplantation, SourceTracker v1.0 [39] was used to estimate the proportional contribution of predefined "source" communities to each "sink". The Source tracker model was trained for individual soil types at different growth periods. The Gibbs sampling was performed with a burn-in of 100 iterations, ten independent restarts, and one valid draw per restart, and a fixed rarefaction depth of 1000 sequences was uniformly applied to all training and test samples. Seedling root

and rhizosphere samples collected 30 days after germination (pre-transplant stage) were designated as primary sources. Rhizosphere and root samples of STC and SYL, harvested at 30, 60 and 90 days post-transplant, were treated as sinks. The unassigned "unknown" fraction represents microbial taxa not detected in any of the predefined source communities (seedling root/rhizosphere).

2.5. Bacterial Isolation and Verification of Pot Experiments

To evaluate the impact of a keystone taxa on the medicinal ingredient content, the bacteria from both the rhizosphere and root of transplanted *Astragalus* were isolated following Haiyambo et al.'s method [40]. Briefly, 1.0 g of rhizosphere soil or 0.5 g of surface-sterilized root tissue was serially diluted (10^{-1} to 10^{-6}) in sterile normal saline (0.85% NaCl). Dilutions were plated on tryptone soy agar (TSA) and R2A agar and incubated at 28 °C for 48–72 h. A total of 411 purified colonies (204 from R2A agar and 207 from TSA were selected based on colony morphology (color, shape and size) and subjected to 16S rRNA gene sequencing. The universal primer pair 27F/1492R (5′-GGTTACCTTGTTACGACTT-3′/5′-AGAGTTTGATCCTGGCTCAG-3′) was amplified for subsequent identification [41]. The amplified products were sequenced and aligned at the National Center for Biotechnology Information (https://www.ncbi.nlm.nih.gov/) using BLAST.

Spearman correlations identified bacterial genera whose abundance was significantly correlated with medicinal ingredient content; these taxa were treated as candidate promoters of secondary metabolite accumulation and used for constructing SynComs. For the pot assay, we followed Wang et al. [42]. Each bacterial strain was grown to OD_{600} 0.8 in LB medium (28 °C, 150 rpm, and 24–48 h), harvested by centrifugation (5000 rpm, 10 min, and 4 °C), washed twice and resuspended in sterile water to OD_{600} 0.8. Equal volumes of bacterial suspension were mixed immediately to obtain SynComs. Each planting bag was filled with 500 g of 3:1 (*v*/*v*) soil–vermiculite mix and autoclaved for 1 h. *Astragalus* seeds were surface-sterilized as described in Section 2.2 and then incubated on sterile, moist filter paper in Petri dishes for 2–3 d until germination. Six uniformly germinated seedlings were transferred to each planting bag and immediately inoculated with SynComs; control bags received the same volume of sterile water. The experiment consisted of four treatments with six biological replicates each: STC soil + SynComs inoculation (Syn-TC); STC soil + sterile water (CK-TC); SYL soil + SynComs inoculation (Syn-YL); and SYL soil + sterile water (CK-YL). Planting bags were randomized within the greenhouse to minimize positional effects. SynComs were re-inoculated twice at 7-day intervals to ensure successful colonization. Plants were grown for 60 days in a greenhouse (25 ± 2 °C; 16 h light/8 h dark), after which plant height, root length and medicinal ingredient content were measured.

2.6. Determination of Astragaloside and Flavonoid Content

Astragaloside (I, II, III and IV) and flavonoid (CA and FO) contents were quantified using a modified method from Xu et al. [43]. The specific measurement method can be found in the Supplementary Materials. Briefly, the root samples were dried and ground into powder, and 0.5 g of root powder was dissolved in methanol, sonicated for 30 min and centrifuged; the supernatant was collected for LC-MS analysis. Stock solutions of astragaloside and flavonoid standards were serially diluted with methanol to 5, 10, 25, 50, 100 and 200 μg mL^{-1} for calibration. The samples and standards were analyzed with a QTRAP5500 LC-MS/MS system (AB SCIEX, Framingham, MA, USA) to determine the medicinal ingredient content.

2.7. Statistical and Data Analysis

All statistical analyses were performed in R v3.6.1. Differences in plant growth parameters, medicinal ingredient contents and alpha-diversity indices were tested via a one-way ANOVA followed by Tukey's HSD ("agricolae" package); significance was set at $p < 0.05$. A two-way ANOVA was used to assess the effects of sampling time and soil type on the medicinal ingredient contents using the "stats" and "car" packages. A linear mixed model was used to identify the major drivers of microbial alpha-diversity with the "lme4" package. The beta-diversity of the bacterial community was assessed via principal coordinate analysis (PCoA) based on the Bray–Curtis distance. The effects of soil type, sampling time and compartment (rhizosphere vs. root) on community structure were tested using permutational multivariate analysis of variance (PERMANOVA) with the adonis2 function ("vegan" package, 999 permutations) and analysis of similarities (ANOSIM) with the anosim function ("vegan" package, 999 permutations). The adonis2 function was used with a full factorial design including soil type, sampling time and their interaction; compartments were included as a fixed factor in separate models for rhizosphere and root communities. The Mantel test was used to estimate correlations between the bacterial community and medicinal ingredient content using the "vegan" package. Differentially abundant ASVs among treatments were identified using EdgeR's generalized linear model (GLM) [44]. Multiple testing correction was applied using the false discovery rate (FDR) method, with significance thresholds set at FDR-adjusted $p < 0.05$ and $|\text{fold-change}| \geq 2.5$. The enrich index (EDI = enrich ASV/depleted ASV) was employed to estimate the microbial enrich efficiency from the seedlings. Random Forest models ("RandomForest" package) were used to identify key microbes driving variation in medicinal ingredient content and plant growth indices. The models included ASV abundances as predictors and medicinal ingredient content/plant growth indices as response variables. Model performance was evaluated using the out-of-bag (OOB) error, and model significance was tested with 5000 permutations of the response variables using the "A3" package.

Spearman correlation analysis was performed using the "corrplot" package to assess the relationships between bacterial genera and medicinal ingredient content/plant growth indices ($p < 0.05$) [45]. Heatmaps were used to display the correlation analysis. Co-occurrence networks were constructed using the "Hmisc" package, with Spearman's correlation coefficient $|r| \geq 0.7$ and FDR-adjusted $p < 0.01$ to reduce spurious edges. Network topological characteristics (nodes, edges, modularity and average path length) were calculated using the "igraph" package. Keystones were identified based on the within-module connectivity (Zi) and among-module connectivity (Pi) according to Poudel et al. [46]. ASVs that were defined as network hubs, module hubs and connectors were identified as keystones. All figures were generated in R with the "ggplot2" package (version 3.2.1). Phylogenetic trees of bacterial isolates were constructed using MEGA7.0 software.

3. Results

3.1. Comparison of Physical and Chemical Properties in Different Soils

ANOVA revealed that, with the exception of ammonium nitrogen (NH_4^+-N), all measured soil properties differed significantly among the three post-transplant soils (Figure S1). Soil water content (SWC) and pH were the highest in Yangling soil (SYL) ($p < 0.05$), being significantly higher than those in STC and SHY ($p < 0.05$). However, STC contained the greatest contents of total nitrogen (TN), total phosphorus (TP), available potassium (AK), available nitrogen (AN) and nitrate nitrogen (NO_3^--N) ($p < 0.05$).

3.2. The Comparative Analysis of Medicinal Ingredients and Growth Indices

The content of astragaloside and flavonoid in *Astragalus* roots was increased with plant development, but the rate and magnitude of increase varied by compound and soil type (Figures 2a,b, S2 and S3). ANOVA revealed that the content of ASTI in *Astragalus* transplanted into STC was significantly higher than that in SHY and SYL in T3 growth period ($p < 0.05$), and the content of AST IV was significantly higher in STC and SYL than that in SHY ($p < 0.05$) (Figure 2a). At T2 and T3, SYL-transplanted *Astragalus* had significantly higher CA and FO contents than SHY and STC ($p < 0.05$) (Figure 2b). Two-way ANOVA revealed that plant growth time, soil type and their interactions had significant effects on the content of medicinal ingredients. Effect sizes (eta-squared, η^2) indicated that the effect of growth time on the content of medicinal ingredients ($\eta^2 = 0.62–0.78$) of *Astragalus* was greater than that of soil type ($\eta^2 = 0.15–0.28$), confirming that plant development is the primary driver of metabolite accumulation (Table S2). Comparative analysis of plant growth indices revealed that the fresh weight and dry weight of plants transplanted in SHY were significantly lower than those in STC and SYL at T2 and T3 ($p < 0.05$) (Figure 2c). The stem length of plants that grew in STC was significantly higher than that in SHY and SYL at T1 ($p < 0.05$) (Figure 2c). The root length of plants that grew in SYL was significantly higher than that in STC and SHY at T2 ($p < 0.05$) (Figure 2c). Similarly, two-way ANOVA reflected that both growth time and soil type significantly affected the plant growth indices ($p < 0.05$), except for fresh weight, dry weight and stem length ($p > 0.05$) (Table S2).

3.3. Root-Associated Microbial Composition in Post-Transplant Plant

At the phylum level, *Proteobacteria*, *Actinobacteriota*, *Acidobacteriota*, *Bacteroidota* and *Gemmatimonadota* were the most dominant phyla in the rhizospheric bacterial community, which accounted for almost 90% of total relative abundance (Table S3). The abundance of most phyla in three soils displayed noteworthy differences in the third growth stage, except for Firmicutes. At T3, the abundances of *Gemmatimonadota*, *Bacteroidota*, *Myxococcota* and *Chloroflexi* increased in SYL ($p < 0.05$), and the abundance of *Actinobacteria* increased in SHY compared to the control (STC) ($p < 0.05$). However, the abundance of Nitrospirota decreased in SHY and SYL compared to the control ($p < 0.05$). While *Proteobacteria* and *Actinobacteria* were the primary phyla accounting for > 94% in the root bacterial community, there were no significant differences in the abundance of dominant phyla among STC, SYL and SHY except for *Bacteroidota* ($p > 0.05$) (Table S3).

In the rhizosphere bacterial composition, analysis of bacterial abundance at the family level revealed that the abundance of *Sphingomonadaceae* and *Microbacteriaceae* decreased significantly in SHY compared to STC ($p < 0.05$). At the T3 growth stage, the abundance of *Xanthobacteraceae* increased in SHY, and *Gemmatimonadaceae* and *Nitrosomonadaceae* increased in SYL compared to STC ($p < 0.05$) (Figure 3a). In the root, Rhizobiaceae abundance remained relatively stable after transplantation, with no significant differences among different soil types and growth stages ($p > 0.05$), indicating that Rhizobiaceae is a conserved core taxon in the root of *A. mongholicus*. The abundance of *Comamonadaceae* and *Burkholderiaceae* both declined following transplantation, with no clear differentiation among the three types of soils post-transplant. In contrast, *Pseudonocardiaceae* abundance increased markedly, peaking in STC soil at the T2 growth stage (Figure 3b).

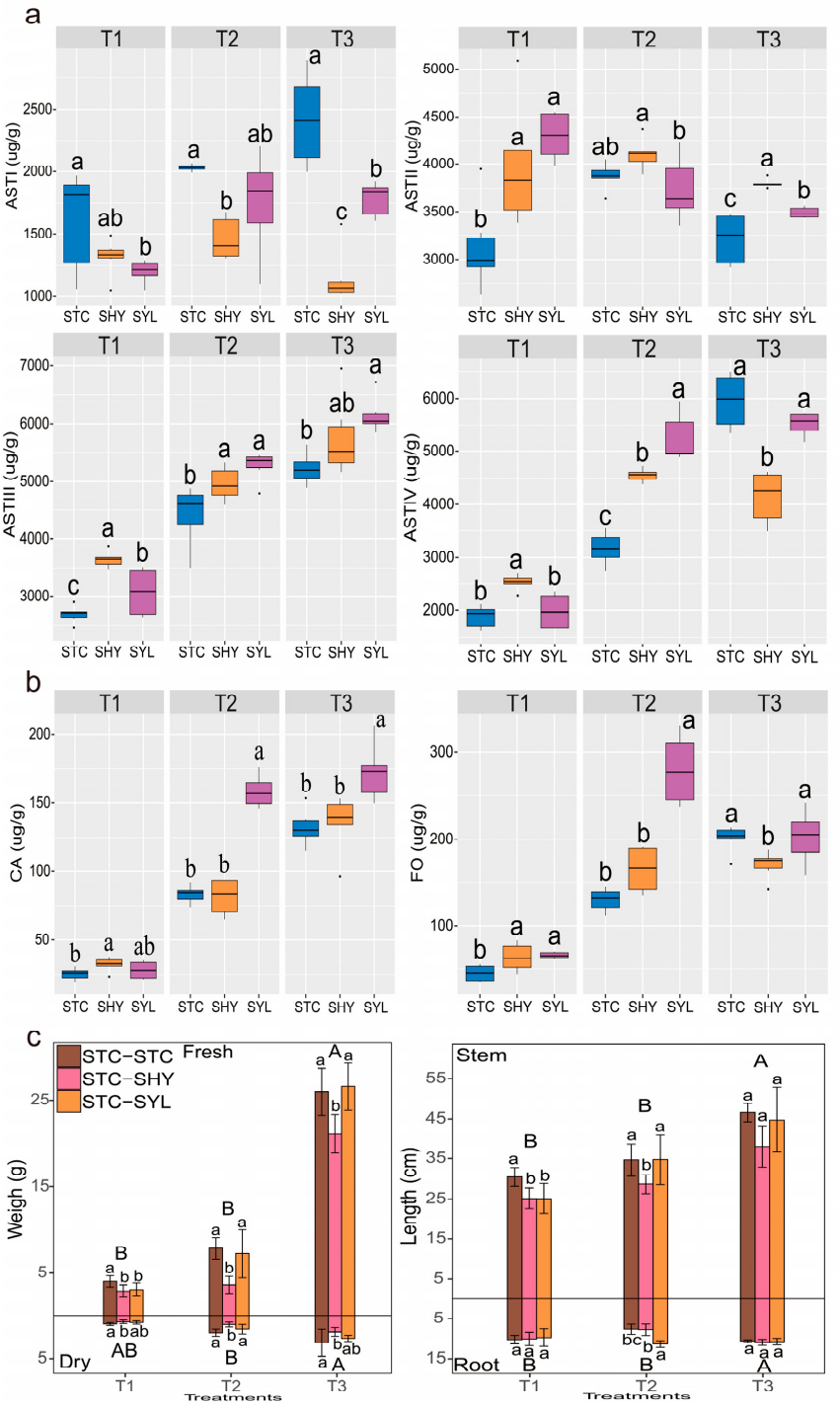


Figure 2. Comparative analysis of medicinal ingredients and plant growth indices. (**a**) Astragaloside content (AST I, AST II, AST III and AST IV) in roots of *Astragalus* transplanted into different soils (STC: Tanchang soil; SHY: Hunyuan soil; and SYL: Yangling soil) at three time points (T1: 30 d, T2: 60 d and T3: 90 d post-transplant). (**b**) Flavonoid content (CA and FO) in roots of *Astragalus* under the same experimental conditions. (**c**) Plant growth indices (fresh weight, dry weight, stem length and root length) of *Astragalus* at T1, T2 and T3 post-transplant. Data are presented as mean ± standard deviation (n = 6). Different letters indicate significant differences between treatments ($p < 0.05$, Tukey's HSD).

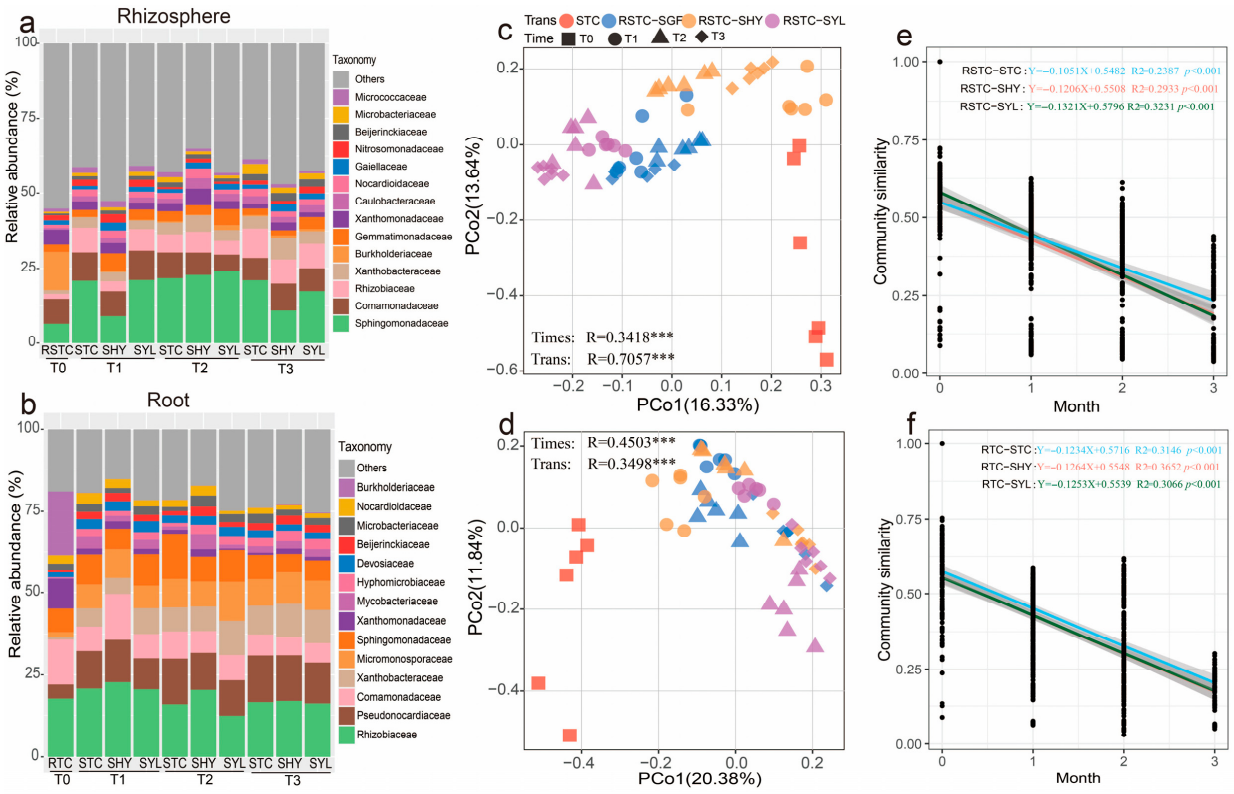


Figure 3. The composition, diversity and community similarity of root-associated microbes. The composition of rhizosphere (**a**) and root (**b**) microbes at the family level in three soils at three periods after transplantation. Principal coordinates analysis (PCoA) based on Bray–Curtis distances displaying a significant difference in the rhizosphere (**c**) and root (**d**) microbes among different soils and sample periods. The community similarity of rhizosphere (**e**) and root (**f**) microbes with the increase in transplantation time. RSTC and RTC indicate the soil before seedling transplantation, STC, SHY and SYL denote the soils into which seedlings were transplanted. T0: seedling stage, T1: 30 d after transplantation, T2: 60 d after transplantation, and T3: 90 d after transplantation. *** represented $p < 0.001$.

3.4. Root-Associated Microbial Diversity in Post-Transplant Soil

Compared to the control, there was no significant change in the alpha-diversity of *Astragalus* rhizosphere bacterial communities (Figure S4 and Table S4). The richness index of root bacterial communities in *Astragalus* transplanted in SHY was lower than that in STC and SYL at the T1 growth stage (Figure S4b). PCoA and ANOSIM analyses revealed that the root-associated bacterial community structure of *A. mongholicus* changed significantly after transplantation, indicating that transplantation is a key factor driving community differentiation (ANOSIM: rhizosphere: R = 0.3418, $p < 0.001$; root: R = 0.4503, $p < 0.001$; Figure 3c,d). ADONIS2 analyses confirmed that plant growth periods significantly structured rhizobacterial communities ($R^2 = 0.2049$, $p < 0.001$) and roots ($R^2 = 0.2768$, $p < 0.001$) (Table S5). PCoA and ANOSIM further showed that transplantation exerted a stronger influence on rhizosphere microbial communities (R = 0.7057) than that of the root (R = 0.3498) (Figure 3c,d). In the time-decay model analysis, the pairwise Bray–Curtis similarity coefficient of root-associated bacterial communities against the time interval between samples was plotted. The slope of the regression equation was estimated via linear regression analysis, and the significance test showed that the slope was significantly less than zero ($p < 0.05$), indicating that the similarity of root-associated bacterial communities decreased significantly with the extension of transplantation time (Figure 3e,f).

The effects of soil type on post-transplant *Astragalus* rhizosphere and root bacterial communities were analyzed separately. ADONIS2 and ANOSIM both showed that each soil type harbored a distinct, tightly clustered community structure. The influence of soil type on rhizosphere communities was most pronounced at the T3 growth period (ADONIS2: $R^2 = 0.5250$, $p < 0.001$; ADOSIM: $R = 0.9885$, $p < 0.001$). In contrast, root bacterial communities were most strongly shaped by soil type at the T2 stage (ADONIS2: $R^2 = 0.4051$, $p < 0.001$; ADOSIM: $R = 0.7749$, $p < 0.001$) (Figure S5). Bray–Curtis dissimilarity was the highest in SHY for both rhizosphere and root communities of post-transplant *Astragalus* (Figure S6), indicating that soil type induced the greatest shift in microbial composition.

3.5. Identification of Key Microbial Strains

Differential ASV analysis between pre- and post-transplant rhizosphere bacterial communities revealed a progressive increase in the number of significantly enriched ASVs as plants grew. Among the three soils, plants in SYL harbored the greatest number of differential ASVs relative to the pre-transplant *Astragalus*, followed by STC and SHY (Figure 4a). The enrichment and depletion pattern of ASVs in *Astragalus* root was similar to that in the rhizosphere, with 289, 260 and 332 ASVs enriched in STC, SHY and SYL at the T3 growth stage, respectively (Figure 4b). Venn analysis revealed that the numbers of rhizosphere ASVs co-enriched across all three soils were 9, 5 and 36 at T1, T2 and T3, respectively, whereas the co-enriched root ASVs were 47, 22 and 97 (Figure S7a). Co-enriched rhizosphere ASVs in STC were dominated by *Proteobacteria*, *Actinobacteria* and *Gemmatimonadota*, whereas those shared by SHY and SYL were almost exclusively *Proteobacteria*. In roots, the consistently enriched ASVs across all three soils belonged mainly to *Proteobacteria* and *Actinobacteria* (Figure S7b).

Co-occurrence networks revealed that rhizosphere bacterial networks were consistently more complex than those in roots, exhibiting more nodes and edges, longer average path lengths and higher modularity; furthermore, >80% of all interactions were positive in every network. Topological characteristic comparison showed that rhizosphere and root networks in SHY displayed the highest complexity and connectivity among the three soils (Figure 4c and Table S6). Moreover, the more intricate rhizosphere networks harbored a greater number of keystone species than the simpler root networks (Tables S6 and S7). Within the rhizosphere co-occurrence network of SYL soil, the seven key ASVs comprised four *Proteobacteria* (*Sphingomonas*; two ASVs, *Sphingomonadaceae* and *Nitrosomonadaceae*), two *Actinobacteriota* (OLB17 and *Acidimicrobiia*) and one *Myxococcota* (Polyangiales). In STC, five ASVs were classified as the keystones and belonged to *Proteobacteria* (*Variovorax*), *Actinobacteriota* (*Actinoplanes*, IMCC26256) and *Bacteroidota* (*Chitinophagaceae*, 2 ASVs). In SHY soil, 18 keystones belonged to *Proteobacteria* (10 ASVs), *Actinobacteriota* (6 ASVs), Firmicutes (1 ASV) and *Acidobacteriota* (1 ASV) (Table S7). In root co-occurrence networks, three key nodes in STC were identified and belonged to *Proteobacteria* (*Nordella* sp.), *Actinobacteriota* (*Pseudonocardia*) and *Actinobacteria*. In SHY soil, 11 keystones belonging to *Proteobacteria* (6 ASVs), *Actinobacteriota* (4 ASVs) and *Patescibacteria* (1 ASV) (Table S8).

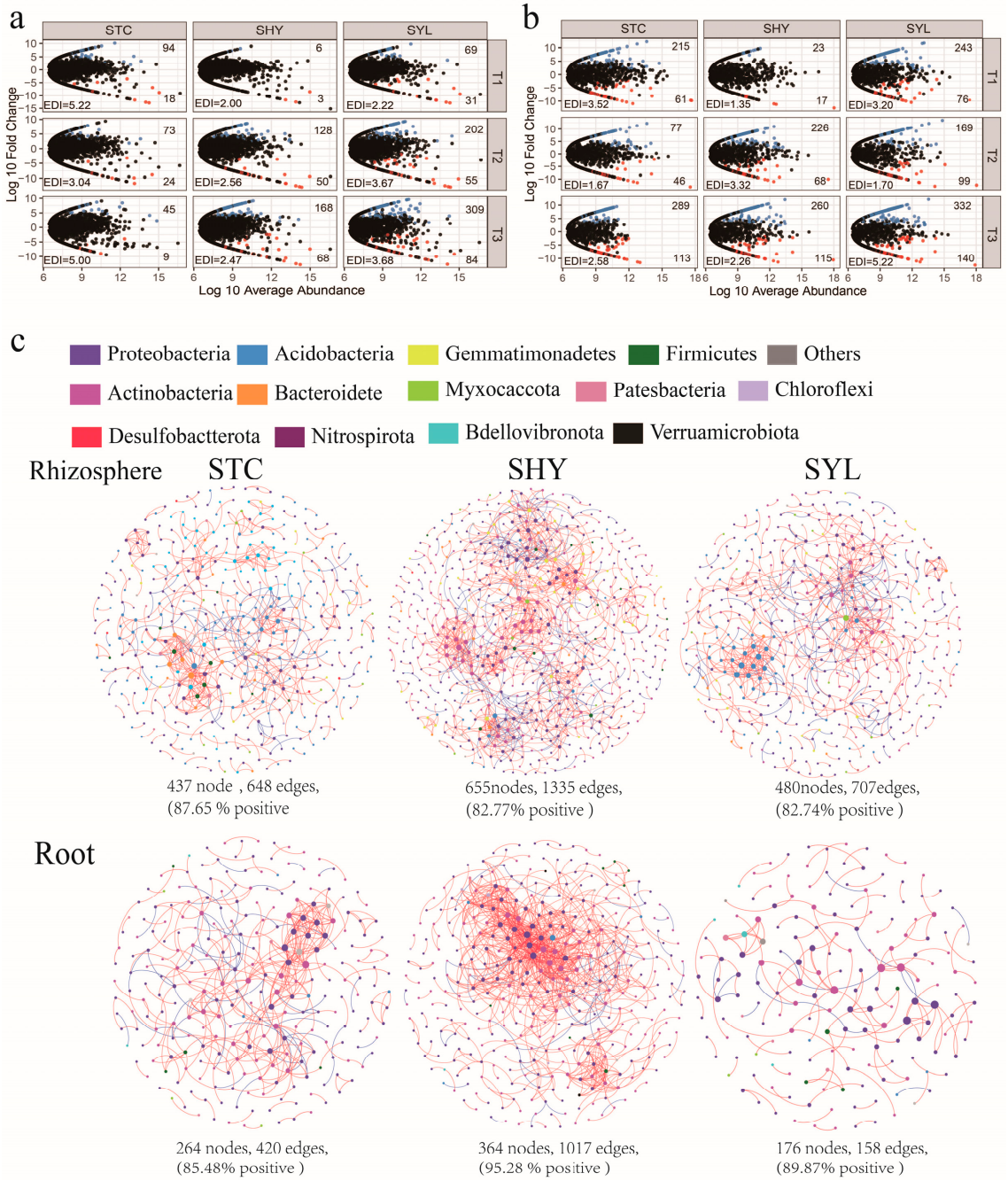


Figure 4. Differential species and network analysis of root-associated microbes. (**a**,**b**) Differential species based on discriminating ASVs (fold change $\geq$ 2.5 and significance test $p < 0.05$). The numbers represent the enriched or depleted ASVs. Blue dots represented the enriched ASVs and red dots reprensented the depleted ASVs. (**c**) Co-occurrence networks were based on the rhizosphere (upper) and root (below) microbes. Red represents positive correlations, and blue represents negative correlations.

3.6. Relationship Between Root-Associated Microbes and Medicinal Ingredients

Mantel tests and MRM linear regression both revealed that post-transplant *Astragalus* rhizosphere bacterial communities were significantly correlated with medicinal ingredient contents ($p < 0.001$; Table 1), and the strongest association was observed in SYL soil (Mantel: $R^2 = 0.6088$; MRM: $R^2 = 0.5252$; $p < 0.001$) (Table 1). In roots, a significant community–metabolite correlation was detected only for plants grown in STC soil (Mantel: $R^2 = 0.4134$; MRM: $R^2 = 0.3783$; $p < 0.001$) (Table 1). Random Forest modeling indicated that there was

a significant association among rhizosphere bacterial communities in SYL soil, medicinal ingredient content and plant growth indices, with the model explaining 63.5% of the variance for medicinal ingredient content and 53.1% of the variance in plant growth indices, with β-diversity emerging as the most influential predictor ($p < 0.05$) (Figure 5a). Root bacterial communities of STC-transplanted *Astragalus* accounted for 75.1% of the variance in medicinal ingredient content and 37.1% of the variance in plant growth indices; equally, β-diversity was the most influential driver ($p < 0.001$) (Figure 5a).

Table 1. Correlation between bacterial community and medicinal ingredients.

Mantel Test	Rhizosphere		Root	
	R	***p***	**R**	***p***
STC	0.5731	<0.0001	0.4134	<0.0001
SHY	0.4635	<0.0001	0.07381	0.2235
SYL	0.6088	<0.0001	0.1266	0.0769
MRM line regression analysis	Rhizosphere		Root	
	R2	*p*	R2	*p*
STC	0.3538	0.0001	0.3783	0.0001
SHY	0.5163	0.0001	0.4275	0.0001
SYL	0.5252	0.0001	0.3261	0.0086

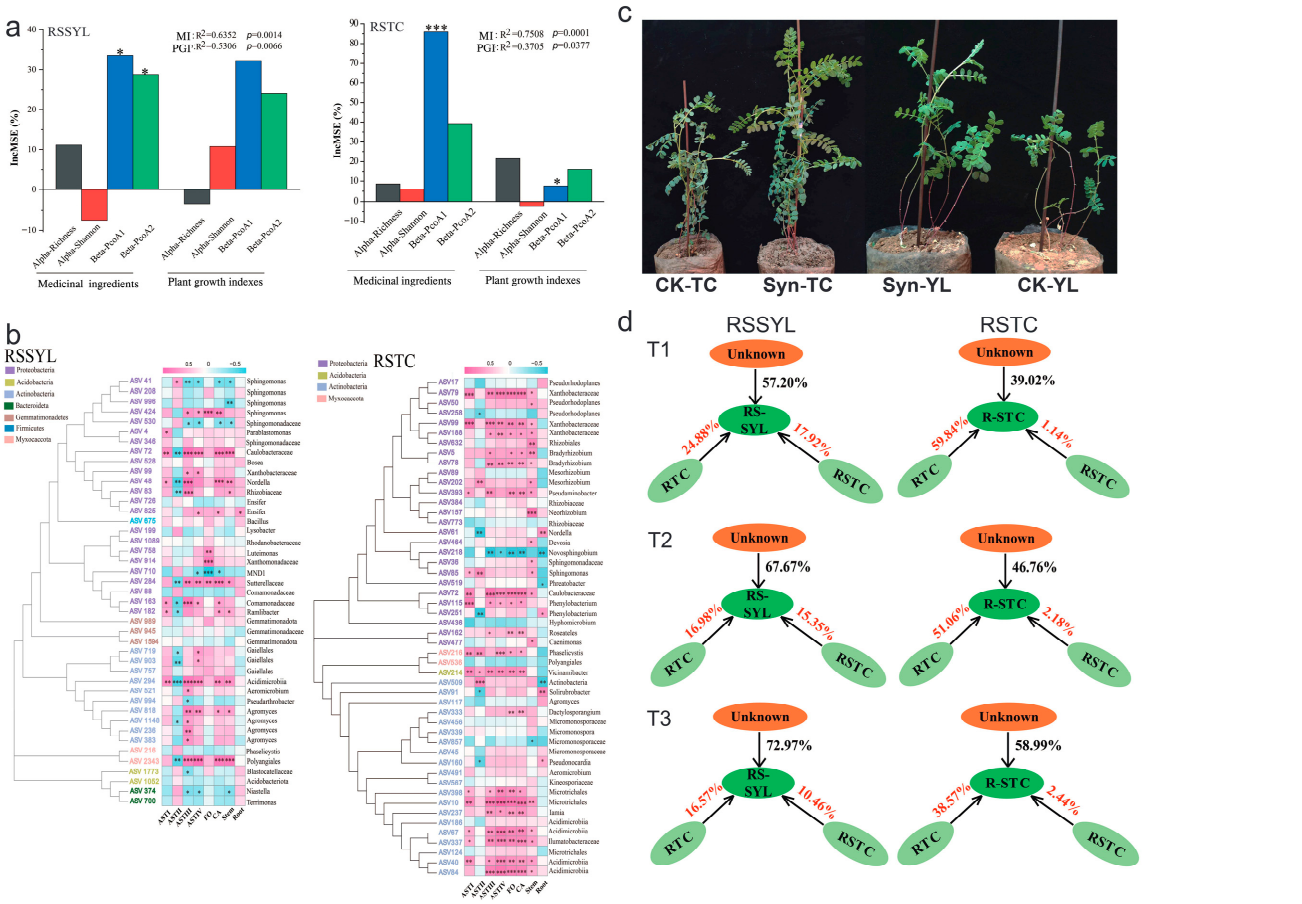


Figure 5. The correlation analysis between the keystone taxa and medicinal ingredients. (**a**) Random Forest model predicting the effects of rhizosphere and root bacterial communities on medicinal ingredients and plant growth. BI represents medicinal ingredients; PP represents plant growth. (**b**) Correlation analysis of key species screened from the rhizosphere and root, and the medicinal

ingredients and plant growth. The evolutionary tree is on the left, and the correlation heatmap is on the right, with different colors representing different phyla. (**c**) Phenotypes of *Astragalus* inoculated with SynComs after 60 days of growth in a greenhouse. (**d**) Source track analysis of microbial communities in the rhizosphere and root transplanted to the SYL and STC. RS-Seedling: Rhizosphere community in seedlings before transplanting; R-Seedling: Root endosphere community in seedlings before transplanting. STC: Soil collected from Tanchang County. SYL: Soil collected from Yangling District. * represented $p < 0.05$; ** represented $p < 0.01$; *** represented $p < 0.001$.

Spearman correlations indicated 40 keystone rhizosphere taxa whose abundances were significantly associated with medicinal ingredient levels. The abundance of ASV_72 (*Caulobacteraceae*) and ASV_294 (*Acidimicrobiia*) was positively correlated with the content of flavonoid, astragaloside and plant height ($p < 0.01$). ASV_424 *(Sphingomonas)*, ASV_758 (*Luteimonas*), ASV_914 (*Xanthomonadaceae*) and ASV_284 (*Sutterellaceae*) can significantly promote the accumulation of formononetin ($p < 0.01$). The 50 keystones in *Astragalus* root in STC were identified as *Proteobacteria* (27), *Acidobacteria* (1), *Actinobacteria* (20) and *Myxococcota* (2). ASV_78 (*Bradyrhizobium*) could increase the contents of ASTIII, ASTI, CA and FO. ASV_202 (*Mesorhizobium*) and ASV_85 (*Sphingomonas*) were significantly correlated with the ASTII content ($p < 0.01$) (Figure 5b).

3.7. Microbial Source Tracking Analysis

SourceTracker analysis showed that seedling-derived microbiota had a persistent impact on post-transplant root-associated bacterial communities, and the contribution rate varied with soil type and growth time. In STC soil, the contribution rates of seedling root endosphere microbiota to post-transplant root communities at T1, T2 and T3 were 59.8%, 51.1% and 38.6%, respectively, while 17.9%, 15.4% and 10.5% were derived from the pre-transplant rhizosphere, showing a gradual decreasing trend (Figure 5d). In SYL soil, the contribution rates of seedling root endosphere microbiota to post-transplant rhizosphere communities at T1, T2 and T3 were 24.9%, 17.0% and 16.6%, respectively (Figure 5d). These results indicated that the priority effect of seedling-derived microbiota was soil-dependent, and its influence gradually weakened with the extension of transplanting time. Meanwhile, the rhizosphere bacteria from SYL-transplanted *Astragalus* and root bacteria from STC-transplanted plants were focused on for subsequent experiments.

3.8. SynCom Construction and Functional Verification

To test the impact of the identified keystone taxa on the medicinal ingredient accumulation and plant growth, we isolated 204 bacteria on R2A medium and an additional 207 rhizospheric strains on TSA medium. Based on the preliminary Spearman's test, three rhizosphere isolates—*Caulobacteraceae* (strain 41R-1), *Acidimicrobiia* (strain 5S-1) and *Sutterellaceae* (strain 3S-16)—and three root endophytes—*Bradyrhizobium* (strain 6S-8), *Sphingomonas* (strain 168) and *Mesorhizobium* (strain HZ-66)—potentially correspond to the key taxa. Thus, these six bacteria were selected to construct the synthetic bacterial communities (SynComs). Compared to the control, the stem length of *Astragalus* grown in STC and SYL inoculated with SynComs increased significantly by 18.89% and 31.96%, respectively ($p < 0.05$) (Figure 5c and Table 2). The ASTIV and CAG content in *Astragalus* planted in STC inoculated with SynComs increased by 52.30% and 55.73% ($p < 0.05$). Similarly, inoculation of SynComs increased the ASTI, ASTII, ASTIV and CAG content of *Astragalus* in SYL by 29.38%, 39.04%, 54.97% and 58.98%, respectively ($p < 0.05$) (Table 2). However, SynCom inoculation had no significant effect on the content of AST III in STC soil ($p > 0.05$).

Table 2. Effects of SynComs on plant growth and medicinal ingredients.

Indices	Root		Rhizosphere	
	TC Soil		YL Soil	
	CK	SynB	CK	SynB
Stem Length (cm)	**21.67 ± 2.16 b**	**26.72 ± 1.84 a**	**10.24 ± 0.60 b**	**15.05 ± 2.22 a**
Root Length (cm)	7.98 ± 0.41 a	9.12 ± 2.16 a	**4.59 ± 0.39 b**	**6.50 ± 0.38 a**
ASTI (μg g^{-1} DW)	1310.67 ± 119.75 a	1864.98 ± 184.48 a	**1065.98 ± 97.72 b**	**3290.69 ± 169.29 a**
ASTII (μg g^{-1} DW)	1206.20 ± 9.42 a	1599.09 ± 155.74 a	1446.86 ± 155.12 a	2573.23 ± 125.67 a
ASTIII (μg g^{-1} DW)	909.18 ± 81.34 a	1264.90 ± 206.91 a	**1013.68 ± 119.43 b**	**1662.99 ± 292.98 a**
ASTIV (μg g^{-1} DW)	**106.08 ± 5.19 b**	**222.42 ± 24.95 a**	**145.86 ± 32.53 b**	**323.92 ± 24.94 a**
CAG (μg g^{-1} DW)	**2.51 ± 1.33 b**	**5.67 ± 0.44 a**	**4.36 ± 1.55 b**	**10.63 ± 0.45 a**

Note: CAG represents Calycosin-7-glucoside. Bold represents the significant difference. *Astragalus* were grown for 60 d after Syncom inoculation. Different letters indicate significant differences between treatments ($p < 0.05$, Tukey's HSD).

4. Discussion

4.1. Post-Transplant Soil Type Drives Both Microbial Assembly and Medicinal Ingredient Profiles

In this study, we mimicked field transplantation of *Astragalus* to track microbiota shifts and their consequences for medicinal metabolites. Soil type was found to exert a profound influence on the chemical composition of medicinal plants via multiple interconnected factors, corroborating previous reports that edaphic context is a primary driver of microbial community assembly in medicinal plants [11,47]. STC soil had the highest TN, TP, AK and AN contents, which likely contributed to the higher astragaloside accumulation in *Astragalus* transplanted into STC. Nitrogen is a key component of the amino acids and enzymes involved in terpenoid biosynthesis, and phosphorus plays a critical role in energy metabolism and signal transduction during secondary metabolite production [12]. In contrast, SYL soil had the highest SWC and pH, which may have favored the growth of flavonoid-promoting rhizosphere bacteria (e.g., *Gemmatimonadota* and *Bacteroidota*). Soil pH and SWC affect nutrient bioavailability and microbial community structure, which in turn modulate plant secondary metabolism [48]. In addition, the chemical profile of *Astragalus* was associated with the detection method. For example, Xu et al. [43] quantified astragalosides in *Astragalus* spp. using HPLC with atmospheric pressure chemical ionization (APCI), whereas our study employed ESI in positive ion mode with multiple reaction monitoring (MRM), which offers higher sensitivity and specificity for the detection of triterpenoid saponins and flavonoids.

Comparative profiling revealed that Nitrospirota was significantly enriched in STC, most likely reflecting the high TN content at this site. Nitrospirota is a widely distributed phylum whose members catalyze the metabolism of nitrite [12] and have been identified as key drivers of both nitrification and denitrification in nitrogen-rich soils. In this study, the abundances of *Gemmatimonadota*, *Bacteroidota*, *Myxococcota* and *Chloroflexi* in the rhizosphere of *A. mongholicus* transplanted into SYL soil were significantly increased. Notably, *Gemmatimonadota*—typically comprising 1–2% of soil bacteria—has been positively linked to elevated total carbon, nitrogen and phosphorus levels, suggesting a nutrient-driven enrichment pattern in this soil [49]. *Bacteroidota* are well-established as dominant carbohydrate degraders that decompose complex soil organics [50], while *Myxococcota* can alter nutrient cycling through extensive predation on other functional bacteria [51]. *Chloroflexi* has been implicated in carbon turnover via community genomic analyses of sediments [52]. Collectively, the enrichment of these taxa suggests that their coordinated participation in soil C-, N- and P-cycling may underlie both enhanced plant growth and increased accumulation of medicinal metabolites. However, the specific functions of these taxa in the

soil used in this experiment need to further be verified via functional gene detection and in vitro culture experiments.

4.2. Priority Effects of Seedling-Stage Colonizers Persist After Transplantation

Microbial source tracking has proven powerful in habitats ranging from urban rivers [53] and gray sufu [54] to plant compartments [55]. Applying the same approach here, we showed that seedling root microbiota remained an important source post-transplant, supplying > 40% of the root community of *Astragalus* in STC but only ~20% of the rhizosphere community of *Astragalus* in SYL, underscoring that the priority effect of seedling-derived microbiota is soil-dependent. Although the plants in SYL had less seedling-derived microbes, this value aligns with previous reports—for example, Luo et al. [56] traced only 15.7% of soybean rhizosphere microbes back to the root zone. The difference in microbial source proportions likely reflects divergent edaphic filters: each post-transplant soil imposes its own selective force, amplifying or diluting the seedling microbiota to different extents [57,58]. Soil and the rhizosphere are the primary reservoirs of endophytes in roots [59]; however, root selectivity typically reduces diversity from bulk soil to the endosphere [57]. Here, although post-transplant soil type strongly filtered root communities, Rhizobiaceae—having established early in seedling roots—maintained a remarkably stable abundance across all subsequent soils. Relevant studies confirm that Rhizobiaceae behave as a conserved core taxon: their abundance remained stable across contrasting soils, underscoring their evolutionarily conserved adaptation to the plant environment [59,60]. In our study, *Bradyrhizobium* sp. and *Mesorhizobium* sp.—both identified as root keystone taxa—are important members of the root-associated microbiota of *A. mongholicus* and were significantly positively correlated with plant biomass and medicinal ingredient content. Previous studies have shown that these two genera are known modulating symbionts of *Astragalus*, reinforcing their dual role in nitrogen fixation and metabolite enhancement [61,62]. Therefore, we speculate that these two genera may improve plant nitrogen nutrition status by fixing nitrogen, thereby promoting plant growth and medicinal ingredient accumulation. However, this is only a hypothetical mechanism, and further experiments, such as ^{15}N isotope tracing and nitrogenase activity determination, are needed to verify it.

Unlike conventional single-strain or filtered inocula, we transplanted the intact root and rhizosphere community, thereby preserving both taxonomic and functional integrity as the plants encountered the new soil environment. Whenever environmental conditions shift, priority effects rapidly re-assert themselves, provided vacant niches and resources remain [63]; this principle must therefore be central to any attempt to integrate microbial consortia across contrasting soils [64]. Moreover, the seedling root microbiota transplanted into STC versus SYL produced divergent downstream communities and metabolite profiles—an observation consistent with ecological theory that environmental filtering amplifies priority effects when microbiota is moved into new habitats [65]. We therefore attribute these differences to the combined action of soil-type filtering and subsequent plant selection.

4.3. Synthetic Bacteria Promote the Accumulation of Medicinal Ingredients and Improve Plant Growth

Enriched taxa and keystones identified here are regarded as potential "ecological steering wheels": by dictating community assembly and core functions, they act as bidirectional mediators between the host plant and its microbiome [58]. Consequently, prioritizing these keystone taxa is becoming essential for selecting microbial strains that serve as effective, reliable inoculants in sustainable agriculture [59]. These taxa are putative keystone taxa based on network topology. A subset of these taxa was selected to construct synthetic communities, and their ability to promote the accumulation of medicinal ingredients in *A. mongholicus* was verified by pot experiments. Here, besides *Bradyrhizobium* and *Mesorhizobium*,

SynComs—comprising *Caulobacteraceae*, *Acidimicrobiia* and *Sutterellaceae*—significantly enhanced both *Astragalus* biomass and medicinal ingredient accumulation ($p < 0.05$). Previous studies have reported that *Caulobacteraceae* and *Acidimicrobiia* are involved in soil nutrient cycling processes [65,66]. In this study, SynCom inoculation significantly promoted plant growth and medicinal ingredient accumulation, which may be related to the improvement of soil nutrient availability by these strains. *Sphingomonas* was previously shown to colonize grapevines and reprogram their secondary metabolism, which may likewise enhance the plant's capacity to accumulate medicinal compounds [67,68]. In addition, some of these ASVs are putative keystone taxa based on Zi/Pi framework in network topology, which may lead to spurious co-occurrence edges and affect the accuracy of keystone identification to a certain extent, therefore more robust and specialized methods for compositional microbial data, such as SparCC and SPIEC-EASI, could be employed to construct more reliable co-occurrence networks in future work.

The synthetic community constructed in this study is a multi-strain consortium, and there may be synergistic or antagonistic interactions among different strains. For example, *Bradyrhizobium* and *Mesorhizobium* may complement each other in nitrogen fixation, while *Caulobacteraceae* and *Acidimicrobiia* may jointly promote nutrient cycling. In future studies, we can further simplify the synthetic community and conduct pairwise combination experiments to clarify the contribution of each strain to plant growth, medicinal ingredient accumulation and the interaction among strains.

5. Conclusions

In this study, through pot experiments, we revealed the dynamic changes in root-associated bacterial communities of *A. mongholicus* after transplantation and their regulatory effect on medicinal ingredient accumulation. The main conclusions are as follows: (1) transplantation into different soils significantly reshaped the structure of root-associated bacterial communities of *A. mongholicus*, and soil type has a stronger shaping effect on rhizosphere communities than on root communities. (2) Seedling-derived microbiota exerted persistent priority effects on post-transplant root-associated bacterial communities, and the strength of the priority effect is soil-dependent. (3) The synthetic community constructed from putative keystone taxa could significantly promote the growth of *A. mongholicus* and the accumulation of medicinal ingredients in a controlled environment. This study clarifies the relationship between root-associated bacterial communities and medicinal ingredient accumulation of *A. mongholicus* after transplantation and provides a theoretical basis for the application of microbial technology in the cultivation of medicinal plants. Future studies should broaden the research scope to include multiple microbial groups and host genotypes, with field experiments conducted to verify the efficacy of synthetic communities.

Supplementary Materials: The following supporting information can be downloaded at https://www.mdpi.com/article/10.3390/microorganisms14020451/s1, Figure S1. The comparative analysis of physical and chemical properties in different soils. Figure S2. Comparison of chromatograms of flavonoid and standard substances. Figure S3. Comparison of chromatograms of saponin and standard substances. Figure S4. Alpha diversity analysis of root-associated microbes in different soil at three plant growth stage. Figure S5. Principal Coordinate analysis (PCoA) based on Bray-Curtis distances displaying the difference of the bacterial community in rhizosphere and root at different growth period. Figure S6. The comparative analysis of Bray-Curtis dissimilarity in rhizosphere and root. Figure S7. The differentially abundant ASV analysis. Table S1. The sampling design during the transplantation process in the experiment. Table S2. Two-way analysis of variance (ANOVA) assessed the effects of growth time and post-transplanted soil on medicinal ingredients and plant growth. Table S3. The rhizosphere and root microbial composition comparison at phylum level in different transplanting time and soil. Table S4. Effects of soil and plant compartments on bacterial

alpha diversity by linear mixed model analysis. Table S5. The effects of plant growth stage and post-transplanted soil on microbial communities in rhizosphere and root based on Bray-Curtis distance. Table S6. Topological characteristics of microbial network in rhizosphere and root after transplanted. Table S7. The keystone of rhizosphere co-occurence network in post-transplanted *Astragalus*. Table S8. The keystone of root co-occurence network in post-transplanted *Astragalus*.

Author Contributions: Y.L. wrote and edited the original draft; Y.L., J.H., X.W. and C.W. conducted the experiments; Z.L. and G.W. conceived of the study, and reviewed and edited the final text. All authors have read and agreed to the published version of the manuscript.

Funding: This study was supported by the National Natural Science Foundation of China (grant No. 42277317) and Shaanxi Province Technology Innovation Guidance Project (grant No. 2025QCY-KXJ-035).

Institutional Review Board Statement: Not applicable.

Informed Consent Statement: Not applicable.

Data Availability Statement: The original contributions presented in this study are included in the article/Supplementary Materials. Further inquiries can be directed to the corresponding author.

Conflicts of Interest: The authors declare no conflicts of interest.

Abbreviations

The following abbreviations are used in this manuscript:

SWC	Soil water content
TP	Total phosphorus
TN	Total nitrogen
AK	Available potassium
AN	Available nitrogen
ASTI	Astragaloside I
ASTII	Astragaloside II
ASTIII	Astragaloside III
ASTIV	Astragaloside IV
CA	Calycosin
FO	Formononetin
CAG	Calycosin-7-glucoside

References

1. Wang, M.; Ge, A.H.; Ma, X.; Wang, X.; Xie, Q.; Wang, L.; Song, X.; Jiang, M.; Yang, W.; Murray, J.D.; et al. Dynamic root microbiome sustains soybean productivity under unbalanced fertilization. *Nat. Commun.* **2024**, *15*, 1668. [CrossRef] [PubMed]
2. Trivedi, P.; He, Z.; Van Nostrand, J.D.; Albrigo, G.; Zhou, J.; Wang, N. Huanglongbing alters the structure and functional diversity of microbial communities associated with citrus rhizosphere. *ISME J.* **2012**, *6*, 363–383. [CrossRef] [PubMed]
3. Trivedi, P.; Trivedi, C.; Grinyer, J.; Anderson, I.C.; Singh, B.K. Harnessing host-vector microbiome for sustainable plant disease management of phloem-limited bacteria. *Front. Plant Sci.* **2016**, *7*, 1423. [CrossRef] [PubMed]
4. Xing, J.; Peng, L.; Chen, J.; Huang, J.; Jiang, P.; Qin, H. A new insight into spacing patterns of soil bacterial microbiome induced by root rot of *Carya cathayensis*. *Appl. Soil Ecol.* **2022**, *174*, 104416. [CrossRef]
5. Zhang, G.; Wei, F.; Chen, Z.; Wang, Y.; Zheng, Y.; Wu, L.; Chen, S.; Dong, L. Rare biosphere in cultivated *Panax* rhizosphere shows deterministic assembly and cross-plant similarity. *Ecol. Indic.* **2022**, *142*, 109215. [CrossRef]
6. Naylor, D.; DeGraaf, S.; Purdom, E.; Coleman-Derr, D. Drought and host selection influence bacterial community dynamics in the grass root microbiome. *ISME J.* **2017**, *11*, 2691–2704. [CrossRef]
7. Chen, S.; Waghmode, T.R.; Sun, R.; Kuramae, E.E.; Hu, C.; Liu, B. Root-associated microbiomes of wheat under the combined effect of plant development and nitrogen fertilization. *Microbiome* **2019**, *7*, 136. [CrossRef]
8. Li, H.; La, S.; Zhang, X.; Gao, L.; Tian, Y. Salt-induced recruitment of specific root-associated bacterial consortium capable of enhancing plant adaptability to salt stress. *ISME J.* **2021**, *15*, 2865–2882. [CrossRef]

9. Qiao, Y.; Wang, Z.; Sun, H.; Guo, H.; Song, Y.; Zhang, H.; Ruan, Y.; Xu, Q.; Huang, Q.; Shen, Q.; et al. Synthetic community derived from grafted watermelon rhizosphere provides protection for ungrafted watermelon against *Fusarium oxysporum* via microbial synergistic effects. *Microbiome* **2024**, *12*, 101. [CrossRef]
10. Li, Z.; Bai, X.; Jiao, S.; Li, Y.; Li, P.; Yang, Y.; Zhang, H.; Wei, G. A simplified synthetic community rescues *Astragalus mongholicus* from root rot disease by activating plant-induced systemic resistance. *Microbiome* **2021**, *9*, 217. [CrossRef]
11. Liu, Y.; Li, Y.; Luo, W.; Liu, S.; Chen, W.; Chen, C.; Jiao, S.; Wei, G. Soil potassium is correlated with root secondary metabolites and root-associated core bacteria in licorice of different ages. *Plant Soil* **2020**, *456*, 61–79. [CrossRef] [PubMed]
12. Jiang, Y.; Han, S.; Luo, X. Role of generalists, specialists and opportunists in Nitrospira community assembly in soil aggregates from nearby cropland and grassland areas in a campus. *Appl. Soil Ecol.* **2024**, *198*, 105377. [CrossRef]
13. Bokoliya, S.C.; Dorsett, Y.; Panier, H.; Zhou, Y. Procedures for fecal microbiota transplantation in murine microbiome studies. *Front. Cell. Infect. Microbiol.* **2021**, *11*, 711055. [CrossRef]
14. Jiang, G.; Zhang, Y.; Gan, G.; Li, W.; Wan, W.; Jiang, Y.; Yang, T.; Zhang, Y.; Xu, Y.; Wang, Y.; et al. Exploring rhizo-microbiome transplants as a tool for protective plant-microbiome manipulation. *ISME Commun.* **2022**, *2*, 10. [CrossRef]
15. Lennon, J.T.; Jones, S.E. Microbial seed banks: The ecological and evolutionary implications of dormancy. *Nat. Rev. Microb.* **2011**, *9*, 119–130. [CrossRef] [PubMed]
16. Bulgarelli, D.; Schlaeppi, K.; Spaepen, S.; Ver Loren van Themaat, E.; Schulze-Lefert, P. Structure and functions of the bacterial microbiota of plants. *Annu. Rev. Plant Boil.* **2013**, *64*, 807–838. [CrossRef]
17. Ren, Y.; Xun, W.; Yan, H.; Ma, A.; Xiong, W.; Shen, Q.; Zhang, R. Functional compensation dominates the assembly of plant rhizospheric bacterial community. *Soil Biol. Biochem.* **2020**, *150*, 107968. [CrossRef]
18. Debray, R.; Herbert, R.A.; Jaffe, A.L.; Crits-Christoph, A.; Power, M.E.; Koskella, B. Priority effects in microbiome assembly. *Nat. Rev. Microbiol.* **2022**, *20*, 109–121. [CrossRef]
19. Carlström, C.I.; Field, C.M.; Bortfeld-Miller, M.; Müller, B.; Sunagawa, S.; Vorholt, J.A. Synthetic microbiota reveal priority effects and keystone strains in the *Arabidopsis phyllosphere*. *Nat. Ecol. Evol.* **2019**, *3*, 1445–1454. [CrossRef]
20. Bergmann, G.E.; Leveau, J.H.J. A metacommunity ecology approach to understanding microbial community assembly in developing plant seeds. *Front. Microbiol.* **2022**, *13*, 877519. [CrossRef]
21. Calderón, K.; Spor, A.; Breuil, M.C.; Bru, D.; Bizouard, F.; Violle, C.; Barnard, R.L.; Philippot, L. Effectiveness of ecological rescue for altered soil microbial communities and functions. *ISME J.* **2017**, *11*, 272–283. [CrossRef] [PubMed]
22. Yan, Y.; Klinkhamer, P.G.L.; van Veen, J.A.; Kuramae, E.E. Environmental filtering: A case of bacterial community assembly in soil. *Soil Biol. Biochem.* **2019**, *136*, 107531. [CrossRef]
23. Navarrete, A.A.; Tsai, S.M.; Mendes, L.W.; Faust, K.; de Hollander, M.; Cassman, N.A.; Raes, J.; van Veen, J.A.; Kuramae, E.E. Soil microbiome responses to the short-term effects of Amazonian deforestation. *Mol. Ecol.* **2015**, *24*, 2433–2448. [CrossRef]
24. Schmitz, L.; Yan, Z.; Schneijderberg, M.; de Roij, M.; Pijnenburg, R.; Zheng, Q.; Franken, C.; Dechesne, A.; Trindade, L.M.; van Velzen, R.; et al. Synthetic bacterial community derived from a desert rhizosphere confers salt stress resilience to tomato in the presence of a soil microbiome. *ISME J.* **2022**, *16*, 1907–1920. [CrossRef]
25. Vorholt, J.A.; Vogel, C.; Carlström, C.I.; Müller, D.B. Establishing Causality: Opportunities of Synthetic Communities for Plant Microbiome Research. *Cell Host Microbe* **2017**, *22*, 142–155. [CrossRef]
26. Jing, J.; Garbeva, P.; Raaijmakers, J.M.; Medema, M.H. Strategies for tailoring functional microbial synthetic communities. *ISME J.* **2024**, *18*, wrae049. [CrossRef]
27. Niu, B.; Paulson, J.N.; Zheng, X.; Kolter, R. Simplified and representative bacterial community of maize roots. *Proc. Natl. Acad. Sci. USA* **2017**, *114*, E2450–E2459. [CrossRef]
28. Jorrin, B.; Haskett, T.L.; Knights, H.E.; Martyn, A.; Underwood, T.J.; Dolliver, J.; Ledermann, R.; Poole, P.S. Stable, fluorescent markers for tracking synthetic communities and assembly dynamics. *Microbiome* **2024**, *12*, 81. [CrossRef]
29. Jia, H.M.; Zheng, C.W.; Wu, Y.R.; Wang, H.; Yan, Z.Y. Metabolomic approach reveals the mechanism of synthetic communities to promote high quality and high yield of medicinal plants—Danshen (*Salvia miltiorrhiza* Bge.). *Chem. Biol. Technol. Agric.* **2024**, *11*, 120. [CrossRef]
30. Yang, M.; Li, Z.; Liu, L.; Bo, A.; Zhang, C.; Li, M. Ecological niche modeling of *Astragalus membranaceus* var. *mongholicus* medicinal plants in Inner Mongolia, China. *Sci. Rep.* **2020**, *10*, 12482. [CrossRef]
31. Fu, J.; Wang, Z.H.; Huang, L.F.; Zheng, S.H.; Wang, D.M.; Chen, S.L.; Zhang, H.T.; Yang, S.H. Review of the botanical characteristics, phytochemistry, and pharmacology of *Astragalus membranaceus* (Huangqi). *Phytother. Res.* **2014**, *28*, 1275–1283. [CrossRef]
32. Li, Y.M.; Liu, Y.; Zhang, H.; Yang, Y.; Wei, G.H.; Li, Z.H. The Composition of Root-Associated Bacteria and Fungi of *Astragalus mongholicus* and Their Relationship With the Bioactive Ingredients. *Front. Microbiol.* **2021**, *12*, 642730. [CrossRef]
33. Edwards, J.; Johnson, C.; Santos-Medellín, C.; Lurie, E.; Podishetty, N.K.; Bhatnagar, S.; Eisen, J.A.; Sundaresan, V. Structure, variation, and assembly of the root-associated microbiomes of rice. *Proc. Natl. Acad. Sci. USA* **2015**, *112*, E911–E920. [CrossRef]

34. Bulgarelli, D.; Rott, M.; Schlaeppi, K.; Ver Loren van Themaat, E.; Ahmadinejad, N.; Assenza, F.; Rauf, P.; Huettel, B.; Reinhardt, R.; Schmelzer, E.; et al. Revealing structure and assembly cues for *Arabidopsis* root-inhabiting bacterial microbiota. *Nature* **2012**, *488*, 91–95. [CrossRef] [PubMed]
35. Callahan, B.J.; McMurdie, P.J.; Rosen, M.J.; Han, A.W.; Johnson, A.J.; Holmes, S.P. DADA2: High-resolution sample inference from Illumina amplicon data. *Nat. Methods* **2016**, *13*, 581–583. [CrossRef] [PubMed]
36. Quast, C.; Pruesse, E.; Yilmaz, P.; Gerken, J.; Schweer, T.; Yarza, P.; Peplies, J.; Glöckner, F.O. The SILVA ribosomal RNA gene database project: Improved data processing and web-based tools. *Nucleic Acids Res.* **2013**, *41*, D590–D596. [CrossRef]
37. Beckers, B.; Op De Beeck, M.; Weyens, N.; Boerjan, W.; Vangronsveld, J. Structural variability and niche differentiation in the rhizosphere and endosphere bacterial microbiome of field-grown poplar trees. *Microbiome* **2017**, *5*, 25. [CrossRef]
38. Reitmeier, S.; Hitch, T.C.A.; Treichel, N.; Fikas, N.; Hausmann, B.; Ramer-Tait, A.E.; Neuhaus, K.; Berry, D.; Haller, D.; Lagkouvardos, I.; et al. Handling of spurious sequences affects the outcome of high-throughput 16S rRNA gene amplicon profiling. *ISME Commun.* **2021**, *1*, 31. [CrossRef]
39. Knights, D.; Kuczynski, J.; Charlson, E.S.; Zaneveld, J.; Mozer, M.C.; Collman, R.G.; Bushman, F.D.; Knight, R.; Kelley, S.T. Bayesian community-wide culture-independent microbial source tracking. *Nat. Methods* **2011**, *8*, 761–763. [CrossRef] [PubMed]
40. Haiyambo, D.H.; Chimwamurombe, P.M.; Reinhold-Hurek, B. Isolation and Screening of Rhizosphere Bacteria from Grasses in East Kavango Region of Namibia for Plant Growth Promoting Characteristics. *Curr. Microbiol.* **2015**, *71*, 566–571. [CrossRef]
41. Walker, A.W.; Martin, J.C.; Scott, P.; Parkhill, J.; Flint, H.J.; Scott, K.P. 16S rRNA gene-based profiling of the human infant gut microbiota is strongly influenced by sample processing and PCR primer choice. *Microbiome* **2015**, *3*, 26. [CrossRef]
42. Wang, Z.; Chen, Z.; Kowalchuk, G.A.; Xu, Z.; Fu, X.; Kuramae, E.E. Succession of the Resident Soil Microbial Community in Response to Periodic Inoculations. *Appl. Environ. Microbiol.* **2021**, *87*, e00046-21. [CrossRef]
43. Xu, Q.; Ma, X.; Liang, X. Determination of astragalosides in the roots of *Astragalus* spp. using liquid chromatography tandem atmospheric pressure chemical ionization mass spectrometry. *Phytochem. Anal.* **2007**, *18*, 419–427. [CrossRef]
44. Robinson, M.D.; McCarthy, D.J.; Smyth, G.K. edgeR: A Bioconductor package for differential expression analysis of digital gene expression data. *Bioinformatics* **2010**, *26*, 139–140. [CrossRef]
45. Wei, T.; Simko, V.R. Package "Corrplot": Visualization of a Correlation Matrix (Version 0.84). 2017. Available online: https://github.com/taiyun/corrplot (accessed on 12 December 2023).
46. Poudel, R.; Jumpponen, A.; Schlatter, D.C.; Paulitz, T.C.; Gardener, B.B.; Kinkel, L.L.; Garrett, K.A. Microbiome Networks: A Systems Framework for Identifying Candidate Microbial Assemblages for Disease Management. *Phytopathology* **2016**, *106*, 1083–1096. [CrossRef]
47. Li, L.; Yang, X.; Tong, B.; Wang, D.; Tian, X.; Liu, J.; Chen, J.; Xiao, X.; Wang, S. Rhizobacterial compositions and their relationships with soil properties and medicinal bioactive ingredients in *Cinnamomum migao*. *Front. Microbiol.* **2023**, *14*, 1078886. [CrossRef]
48. Sun, X.; Zhang, X.K.; Zhang, G.S.; Miao, Y.J.; Zeng, T.X.; Zhang, M.; Zhang, H.H.; Zhang, L.; Huang, L.F. Environmental Response to Root Secondary Metabolite Accumulation in *Paeonia lactiflora*: Insights from Rhizosphere Metabolism and Root-Associated Microbial Communities. *Microbiol. Spectr.* **2022**, *10*, e0280022. [CrossRef]
49. Mujakić, I.; Piwosz, K.; Koblížek, M. Phylum *Gemmatimonadota* and its role in the environment. *Microorganisms* **2022**, *10*, 151. [CrossRef] [PubMed]
50. Kruczyńska, A.; Kuźniar, A.; Podlewski, J.; Słomczewski, A.; Grządziel, J.; Marzec-Grządziel, A.; Gałązka, A.; Wolińska, A. *Bacteroidota* structure in the face of varying agricultural practices as an important indicator of soil quality—A culture independent approach. *Agr. Ecosyst. Environ.* **2023**, *342*, 108252. [CrossRef]
51. Zou, D.; Zhang, C.; Liu, Y.; Li, M. Biogeographical distribution and community assembly of *Myxococcota* in mangrove sediments. *Environ. Microbiome* **2024**, *19*, 47. [CrossRef] [PubMed]
52. Hug, L.A.; Castelle, C.J.; Wrighton, K.C.; Thomas, B.C.; Sharon, I.; Frischkorn, K.R.; Williams, K.H.; Tringe, S.G.; Banfield, J.F. Community genomic analyses constrain the distribution of metabolic traits across the *Chloroflexi* phylum and indicate roles in sediment carbon cycling. *Microbiome* **2013**, *1*, 22. [CrossRef]
53. Derx, J.; Kılıç, H.S.; Linke, R.; Cervero-Aragó, S.; Frick, C.; Schijven, J.; Kirschner, A.K.T.; Lindner, G.; Walochnik, J.; Stalder, G.; et al. Probabilistic fecal pollution source profiling and microbial source tracking for an urban river catchment. *Sci. Total Environ.* **2023**, *857*, 159533. [CrossRef] [PubMed]
54. Ding, S.; Tian, M.; Yang, L.; Pan, Y.; Suo, L.; Zhu, X.; Ren, D.; Yu, H. Diversity and dynamics of microbial population during fermentation of gray sufu and their correlation with quality characteristics. *LWT* **2023**, *180*, 114711. [CrossRef]
55. Dove, N.C.; Klingeman, D.M.; Carrell, A.A.; Cregger, M.A.; Schadt, C.W. Fire alters plant microbiome assembly patterns: Integrating the plant and soil microbial response to disturbance. *New Phytol.* **2021**, *230*, 2433–2446. [CrossRef]
56. Luo, W.; Wang, J.; Li, Y.; Wang, C.; Yang, S.; Jiao, S.; Wei, G.; Chen, W. Local domestication of soybean leads to strong root selection and diverse filtration of root-associated bacterial communities. *Plant Soil* **2022**, *480*, 439–455. [CrossRef]
57. Philippot, L.; Raaijmakers, J.M.; Lemanceau, P.; van der Putten, W.H. Going back to the roots: The microbial ecology of the rhizosphere. *Nat. Rev. Microbiol.* **2013**, *11*, 789–799. [CrossRef]

58. Trivedi, P.; Leach, J.E.; Tringe, S.G.; Sa, T.; Singh, B.K. Plant-microbiome interactions: From community assembly to plant health. *Nat. Rev. Microbiol.* **2020**, *18*, 607–621. [CrossRef]
59. Compant, S.; Cassan, F.; Kostić, T.; Johnson, L.; Brader, G.; Trognitz, F.; Sessitsch, A. Harnessing the plant microbiome for sustainable crop production. *Nat. Rev. Microbiol.* **2025**, *23*, 9–23. [CrossRef] [PubMed]
60. Garrido-Oter, R.; Nakano, R.T.; Dombrowski, N.; Ma, K.W.; AgBiome Team; McHardy, A.C.; Schulze-Lefert, P. Modular traits of the Rhizobiales root microbiota and their evolutionary relationship with symbiotic rhizobia. *Cell Host Microbe* **2018**, *24*, 155–167.e5. [CrossRef]
61. Zhao, C.T.; Wang, E.T.; Zhang, Y.M.; Chen, W.F.; Sui, X.H.; Chen, W.X.; Liu, H.C.; Zhang, X.X. *Mesorhizobium silamurunense* sp. nov., isolated from root nodules of *Astragalus* species. *Int. J. Syst. Evol. Microbiol.* **2012**, *62*, 2180–2186. [CrossRef]
62. Yan, H.; Ji, Z.J.; Jiao, Y.S.; Wang, E.T.; Chen, W.F.; Guo, B.L.; Chen, W.X. Genetic diversity and distribution of rhizobia associated with the medicinal legumes *Astragalus* spp. and *Hedysarum polybotrys* in agricultural soils. *Syst. Appl. Microbiol.* **2016**, *39*, 141–149. [CrossRef]
63. Fukami, T. Historical Contingency in Community Assembly: Integrating Niches, Species Pools, and Priority Effects. *Annu. Rev. Ecol. Evol. Syst.* **2015**, *46*, 1–23. [CrossRef]
64. Rillig, M.C.; Antonovics, J.; Caruso, T.; Lehmann, A.; Powell, J.R.; Veresoglou, S.D.; Verbruggen, E. Interchange of entire communities: Microbial community coalescence. *Trends. Ecol. Evol.* **2015**, *30*, 470–476. [CrossRef]
65. Wang, F.; Gao, Y.; Li, X.; Luan, M.; Wang, X.; Zhao, Y.; Zhou, X.; Du, G.; Wang, P.; Ye, C.; et al. Changes in microbial composition explain the contrasting responses of glucose and lignin decomposition to soil acidification in an alpine grassland. *Sci. Total Environ.* **2024**, *930*, 172671. [CrossRef] [PubMed]
66. Zhao, Z.; Pan, Y.; Jiang, J.; Gao, S.; Sun, H.; Dong, Y.; Sun, P.; Guan, X.; Zhou, Z. Unrevealing variation of microbial communities and correlation with environmental variables in a full culture-cycle of *Undaria pinnatifida*. *Mar. Environ. Res.* **2018**, *139*, 46–56. [CrossRef] [PubMed]
67. Lòpez-Fernàndez, S.; Compant, S.; Vrhovsek, U.; Bianchedi, P.L.; Sessitsch, A.; Pertot, I.; Campisano, A. Grapevine colonization by endophytic bacteria shifts secondary metabolism and suggests activation of defense pathways. *Plant Soil* **2015**, *405*, 155–175. [CrossRef]
68. Ludwig-Müller, J. Plants and endophytes: Equal partners in secondary metabolite production? *Biotechnol. Lett.* **2015**, *37*, 1325–1334. [CrossRef]

Disclaimer/Publisher's Note: The statements, opinions and data contained in all publications are solely those of the individual author(s) and contributor(s) and not of MDPI and/or the editor(s). MDPI and/or the editor(s) disclaim responsibility for any injury to people or property resulting from any ideas, methods, instructions or products referred to in the content.